



EUROPEAN
SPALLATION
SOURCE

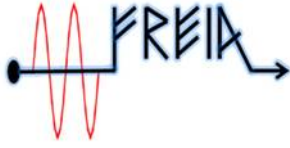
ESS AD Technical Note
ESS/AD/0049

Accelerator Division

**Vitaliy Goryashko, Volker Ziemann,
Tor Lofnes and Roger Ruber**

**The RF Power Consumption in the ESS
Spoke Linac**

16 January 2013



Uppsala University
FREIA Group

16th January 2013

vitaliy.goryashko@physics.uu.se

RF POWER CONSUMPTION IN THE ESS SPOKE LINAC

V. Goryashko, V. Ziemann, T. Lofnes, R. Ruber,
FREIA Group, Uppsala University

Abstract

In the ESS LINAC the transition energy between the DTL and the spoke LINAC was changed by adding the fourth DTL tank in order to match the spoke LINAC in terms of the velocity acceptance. We present calculation of the RF power required to be fed to each spoke cavity to achieve the nominal acceleration gradient. The RF power overhead needed to compensate the beam loading and the Lorentz detuning is calculated and the peak and average values of the total RF power are presented. Overhead in terms of the power averaged over the pulse is only a few percents whereas the peak power overhead can reach 20% and lasts for around 200 microseconds. It turns out that the power overhead is mainly determined by the strong beam loading because of a high beam current whereas the Lorentz detuning is weak due to high stiffness of the spoke cavity and almost does not require extra power to the cavity. In our simulations the cavity voltage and phase are stabilized within nominal tolerances by feedback and feed-forward. A slow feed-forward is used to cure the Lorentz detuning whereas a fast feedback through a signal oscillator is applied to compensate the beam loading effect.

Contents

1	Introduction	3
2	Double Spoke Cavity	3
3	Acceleration in the ESS Spoke LINAC	4
4	The Beam-Cavity Interaction	6
5	Optimum External Quality Factor	9
6	Simulation of a Single Cavity	10
6.1	cavity without control	11
6.2	cavity with control but without pre-detuning	14
6.3	cavity with control and pre-detuning	18
7	RF Power Consumption along the Spoke LINAC	21
8	Conclusion	22
	References	23

1 Introduction

The spoke cavity is a superconducting TEM type resonator with large velocity acceptance and high mechanical stiffness. Although the spoke cavity was invented more than twenty years ago and numerous studies on it have been performed, the ESS LINAC will be the first LINAC using spoke cavities to accelerate the beam. Experience with other types of superconducting cavities indicates that high-power test is vital for reliable operation of the cavity in an accelerator. Therefore, the FREIA group at Uppsala University is building a high-power RF test facility able to study performance of the ESS spoke cavity. In addition, the FREIA RF source is considered as a prototype for the ESS spoke LINAC source. The requirements on an RF source are dictated by the beam-wave interaction in spoke cavities of the ESS LINAC so that in the present report we study in detail the beam-wave interaction in each cavity of the ESS spoke LINAC and calculate the RF power consumption taking into account the beam loading and the Lorentz detuning.

In the previous ESS LINAC design [1] the transition energy between the DTL and the spoke LINAC was chosen to be 50 MeV but the beam velocity corresponding to this energy is on the edge of the double spoke cavity velocity acceptance such that first several cavities of the spoke LINAC were inefficient and an average power up to 400 kW to the coupler had to be provided [2]. Therefore, the ESS LINAC was redesigned and the transition energy between the DTL and the spoke LINAC was increased to 79 MeV by adding the fourth DTL tank in order to match the spoke LINAC in terms of the velocity acceptance. For the new LINAC design we present calculation of the RF power required to be fed to each cavity to achieve the nominal acceleration gradient. The RF power overhead needed to compensate the beam loading and the Lorentz detuning is studied.

To obtain the beam of a high quality in terms of the energy spread and emittance the cavity voltage magnitude and phase should be controlled very accurately. According to the ESS design [1], the voltage magnitude deviation must be below 0.1% of the total value and its phase deviation must not exceed 0.5 degrees. This can be achieved by means of an appropriate control. The most widely used control technique is the negative feedback based on a PID controller. The idea is to control a system's output by comparing it to a desired setpoint and feeding the error back to the input dynamically. At the same time, when a perturbation can be foreseen like the Lorentz detuning, it is useful to use a feed-forward technique to prevent such a perturbation. Combined feedback and feed-forward control can significantly improve performance over simple feedback architectures when there is a major disturbance to the system that can be measured beforehand [3]. In the present study we apply the aforementioned techniques of control to stabilize the cavity voltage magnitude and phase in cavities of the ESS spoke LINAC. Features of the double spoke cavity and the LINAC design are discussed.

2 Double Spoke Cavity

There are three major classes of superconducting structures [4]: high, medium and low- β , where $\beta = v/c$ is the normalized velocity of accelerated particles and c is the speed of light. Medium velocity structures with β between 0.2 and 0.7 are used for protons with energies less than 1 GeV as well as for ions. The cavity gap length is usually $\beta\lambda/2$, where λ is the wavelength corresponding to the frequency choice for the accelerating structure. For $\beta < 0.5$ spoke resonators with single or multigaps are becoming popular due to their large velocity acceptance and mechanical stiffness [5].

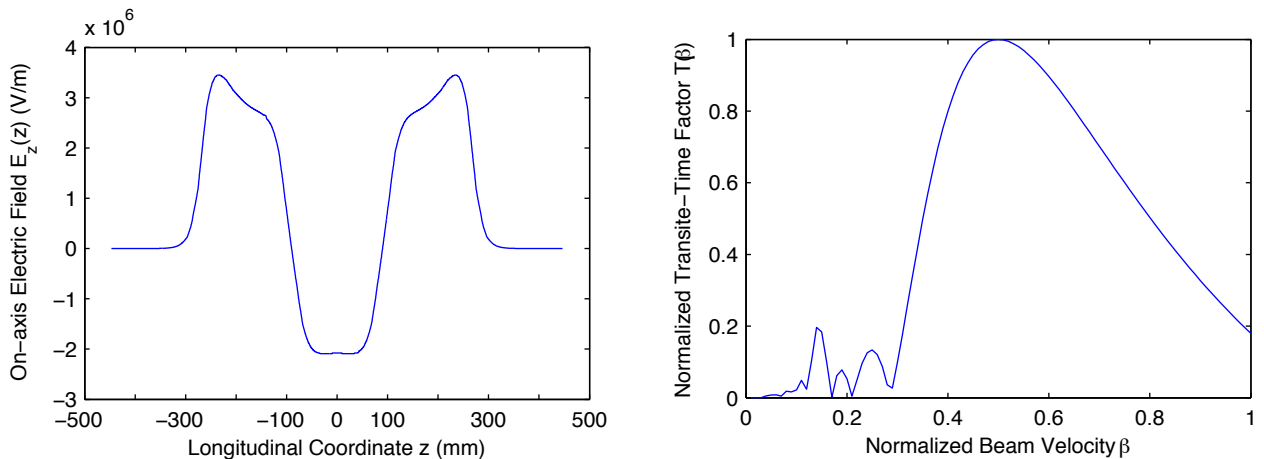


Figure 2.1: The on-axis accelerating electric field as a function of the longitudinal position in the double spoke cavity (on the left). Normalized transire-time factor, $T(\beta)$, vs. beam velocity β (on the right).

Elliptical shape cells for $\beta < 0.5$ become mechanically unstable as the accelerating gaps shortens and cavity walls become nearly vertical. The choice of a low RF frequency, favored for ion and proton applications, also makes the elliptical cells very large.

Spoke resonators belong to the family of TEM resonators and each spoke element can be considered as a half-wavelength resonant transmission line operating in a TEM mode. A half-wavelength transmission line, with a short at both ends, has maximum voltage in the middle and behaves as a half-wavelength resonator. For a multispoke resonator, the electric field of the accelerating mode in adjacent gaps differs in phase by π radians as one can see in Fig. 2.1, where the accelerating electric field of the double spoke is shown ¹. Thus, the name π -mode applies to the accelerating mode that in fact is the lowest frequency mode in the pass-band. Due to the change in the field during the finite time of particles transit across the accelerating gap, a particle of charge q traversing the gap with velocity β has an energy gain lower than qV_g , where V_g is the maximal gap voltage. The transit-time factor integral takes into account the corresponding drop in voltage gain. A typical resonator is optimized for the maximum transit-time factor at a particular β value called the resonator geometrical beta but the transit-time factor will drop for other β values. The normalized transit-time factor $T(\beta)$ for the double spoke resonator designed at IPN Orsay is shown in Fig. 2.1.

3 Acceleration in the ESS Spoke LINAC

To bring the beam to the highest energy within a given length of the ESS spoke LINAC, the spoke cavities are chosen to operate at the same maximal accelerating gradient [6] since it directly determines the maximal energy gain achievable in a cavity. Maximal E_{acc} for a double spoke cavity is 8.5 MV/m and limited by the peak surface electric and magnetic fields (35 MV/m and 70 mT) as well as longitudinal phase advance constrains related to the beam dynamics. The accelerating

¹the authors are thankful to Sebastien Bousson for providing the data

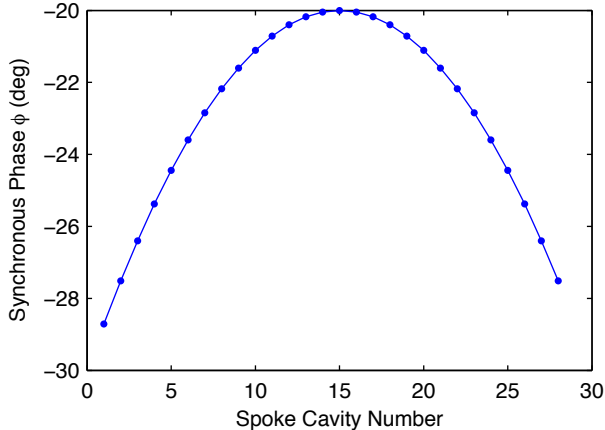


Figure 3.1: The synchronous RF phase ϕ_s along the spoke LINAC.

cavity voltage is related to accelerating gradient E_{acc} by $V_c = E_{acc}L_{acc}$, where $L_{acc} = (n + 1)\beta\lambda/2$ is the accelerating length and n is the number of spoke bars. Note that all characteristics of the cavity are defined for β equaling the cavity geometrical beta. This implies that beams having different velocities will see different accelerating voltages because of different transit-time factors. In addition, the synchronous RF phase changes along the LINAC, thus additionally changing the power transfer to the beam. To achieve a sufficient longitudinal acceptance by longitudinal RF focusing, the synchronous phase starts out at -35° degrees at the beginning of the DTL. The lower space charge forces at the higher energies allows to increase the synchronous phase to -15° towards the end of the medium- β cavities and remains at that value throughout the high- β section [7]. To ensure a smooth phase advance variation across the frequency jump from 352.21 to 704.42 MHz at the end of the spokes, and to capture all particles after the frequency jump, the synchronous phase is in addition decreased towards the end of the spokes. The longitudinal focusing is thus increased, shortening the bunch as a preparation for the frequency jump [7]. The synchronous phase in the spoke LINAC may be approximated by a parabolic function and is shown in Fig. 3.1.

Once defined the normalized transit-time factor the cavity voltage seen by the beam can be written as

$$\Delta V_b(\beta) = \Delta V_b(\beta_{opt})T(\beta) \cos \phi_s, \quad (3.1)$$

where ϕ_s is the synchronous phase of the RF field seen by the beam and $\Delta V_b(\beta_{opt})$ is the maximal cavity voltage seen by the particle accelerated on-crest ($\phi_s = 0$) with β equaling the geometrical beta of the cavity. The beam velocity is assumed to be constant during passing the cavity such that using Eq. (3.1) and definitions for the beam energy, U_b , and velocity

$$\gamma = 1 + (U_b + e\Delta V_b)/(m_p c^2), \quad \beta = \sqrt{1 - 1/\gamma^2}, \quad (3.2)$$

where m_p is the proton mass, one can successively calculate the beam energy along the LINAC. The energy gain $\Delta U_b = e\Delta V_b$ strongly depends on the initial beam energy U_b at the first spoke cavity via the normalized transit-time factor $T[\beta(U_b)]$. This initial energy is the transition energy between the DTL and the spoke cavities. The results of calculation of ΔU_b as a function of U_b are

shown in Fig. 3.2. The maximum ΔU_b of 127 MeV is achieved for an initial energy of 100 MeV. One can also see that the transition energy of 79 MeV between the DTL and the spoke cavities defined in the latest ESS design is a good compromise between the minimum transition energy and maximum energy gain. In what follows this value of the beam energy at the beginning of the spoke LINAC is used for simulations.

The voltage seen by the beam and the beam energy in each cavity of the spoke LINAC are shown in Fig. 3.3. Note that to estimate the beam energy gain along the LINAC one needs to know only the maximal accelerating gradient, the normalized transit-time factor and the synchronous phase distribution along the LINAC. However, to calculate an RF power needed to feed the cavities one has to consider dynamics of the cavity voltage and phase in the presence of the beam loading and Lorentz detuning. This is done in the next section by modeling the cavity and the beam by lumped elements.

4 The Beam-Cavity Interaction

To study the evolution of the accelerating field in a spoke cavity we will adopt the traditional model [8], in which the cavity is presented by a lumped RLC circuit, the coupler by a transmission line with impedance Z_T on which we have the incident (generator) wave current I_i and the reflected wave current I_r , see Fig. 4.1. The latter is assumed to disappear without re-reflection (typically there is a circulator between the spoke cavity and the RF source). The beam is modeled as a current source with current I_b^{RF} , where I_b^{RF} is the RF beam current that is twice of the DC beam current, $I_b^{RF} = 2I_b^{DC}$. The cavity characterized by the angular resonant frequency ω_0 is excited to voltage V_c under these conditions. The geometric shunt impedance (R/Q) of the cavity is defined as

$$(R/Q) = \frac{1}{2} \frac{V_c^2}{\omega_0 U_{st}}, \quad (4.1)$$

where U_{st} is the energy stored in the cavity.

We will assume that variations of the generator and beam currents as well as external pertur-

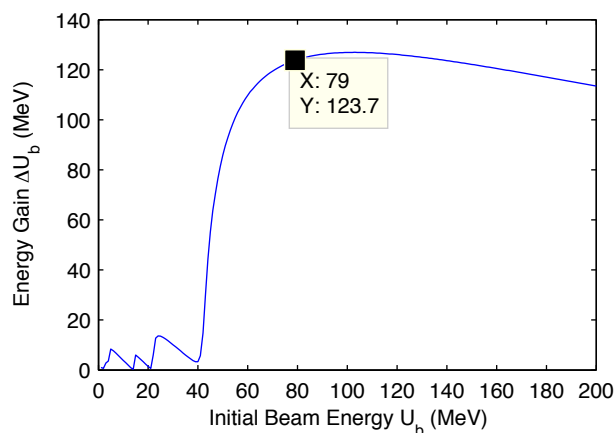


Figure 3.2: The energy gain vs. the transition energy between the DTL and the spoke LINAC.

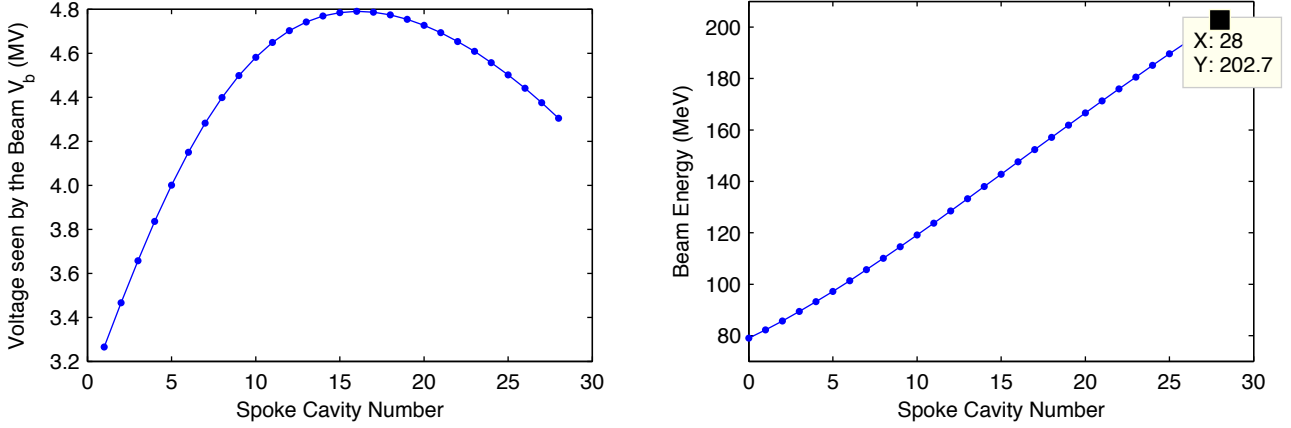


Figure 3.3: The voltage seen by the beam V_b (on the left) and the beam energy U_b (on the right) along the spoke LINAC.

bations are slow as compared to the RF period such that a dynamic quantity may be represented as a product of a slow varying envelope multiplied by $\exp(i\omega t)$ (in general case ω is not identical to ω_0), e.g. $V_c(t) = \text{Re}\{A(t) \exp(i\omega t)\}$ and $\omega^{-1} \text{d} \ln A / \text{d} t \ll 1$. The impedances of the loaded cavity and transmission line can be expressed in terms of the shunt cavity resistance R , and three quality factors: Q_0 is the quality factor of the bare cavity, Q_{ext} is the quality factor of the coupler cavity, $Q_L = (Q_0^{-1} + Q_{ext}^{-1})^{-1}$ is the total quality factor. For a superconducting cavity the loaded quality factor is mainly determined by the external Q -factor, $Q_L \approx Q_{ext}$. Note that Q_{ext} is a way to express the coupling strength of an (RF) coupler: $Q_{ext} P_{ext} = \omega U_{st}$, where P_{ext} is the power leaking out of this coupler for the given U_{st} .

Using the slow varying approximation we arrive at a first order differential equation for the complex cavity voltage amplitude [8]

$$t_F \frac{\text{d}A}{\text{d}t} + A(1 - 2i\delta Q_L) = 2Q_L \frac{R}{Q} [I_i(t) - I_b^{DC}(t) F_b e^{-i\phi_s}], \quad (4.2)$$

where $\delta = (\omega_0 - \omega)/\omega$ is the normalized detuning, ϕ_s is the synchronous phase defined according to the electron linac convention (the energy transfer from the field to the beam is maximal when $\phi_s = 0$), F_b is the beam form-factor, t and $t_F = 2Q_L/\omega$ are the observation and filling time, respectively.

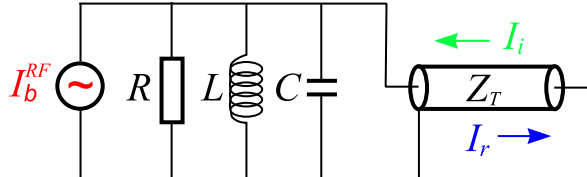


Figure 4.1: The lumped model: cavity modeled by an RLC circuit, the coupler by a connected transmission line of impedance Z_T and the beam by a current source.

The current reflected by the cavity reads

$$I_r(t) = \frac{1}{2Q_L(R/Q)} \left[A(1 + 2i\delta Q_L) - t_F \frac{dA}{dt} \right] - I_b^{DC}(t) F_b e^{-i\phi_s}. \quad (4.3)$$

and the power coming to the cavity from the coupler (incident power) and the power reflected by the cavity to the coupler are

$$P_{i,r} = \frac{R/Q}{2} Q_{ext} |I_{i,r}|^2. \quad (4.4)$$

The energy conservation law reads

$$\frac{1}{t_F} \frac{dU_{st}}{d\tau} = P_g - P_r - P_b, \quad (4.5)$$

where $U_{st} = |A|^2/2\omega Q_L$ is the energy stored in the cavity and

$$P_b = \text{Re}\{AI_{b,DC}^* e^{i\phi_s}\} \quad (4.6)$$

is the power transferred to the beam.

Within the steady-state limit ($A(t) = V_c = \text{const}$) one can minimize the reflected power by tuning the cavity, the so-called ‘reactive beam loading compensation’,

$$\frac{\Delta\omega^{opt}}{\omega} = \frac{(R/Q)I_b^{DC} F_b \cos \phi}{V_c} \quad (4.7)$$

and the reflected power completely disappears if the coupler is also adapted such that

$$Q_{ext}^{opt} = \frac{V_c}{2(R/Q)I_b^{DC} F_b \sin \phi}. \quad (4.8)$$

For a high Q resonator such as superconducting cavities, the narrow electromagnetic bandwidth makes the coupling between the cavity and the RF feeding source sensitive to rather small amount of detuning. As a result, small mechanical deformations due to, for example, the surrounding vibration noise (microphonics) or Lorentz forces (due to the radiation pressure), are a source of concern. Whereas microphonics are usually critical for CW operation, the dynamic detuning associated to Lorentz forces is the main issue for pulsed operation as in the SNS [9]. Then, one can also expect the Lorentz detuning to be especially relevant to the ESS spoke cavity. In the case of the static field pressure the frequency deviation is proportional to the negative square of the accelerating field $\Delta f = -|K_L|E_{acc}^2$, where $K_L < 0$ is referred to as the Lorentz detuning factor in $\text{Hz}/(\text{MV}/\text{m})^2$. If we now take into account only the main mechanical mode, then the frequency deviation may be approximately described by a 1st order differential equation

$$\tau_m \frac{d\Delta\omega}{dt} = -[\Delta\omega(t) - \Delta\omega_T(t)] + 2\pi K_L E_{acc}^2, \quad (4.9)$$

where $E_{acc}^2 = |A|^2/L_{acc}^2$ and $L_{acc} = (n+1)\beta\lambda/2$ are the accelerating electric field and length, respectively, β is the velocity factor, n is the number of spoke bars, λ is the wavelength of the accelerating field, τ_m is the mechanical damping time constant and $\Delta\omega_T(t)$ is a frequency shift due to an external mechanical excitation (such as a piezo-electric tuner).

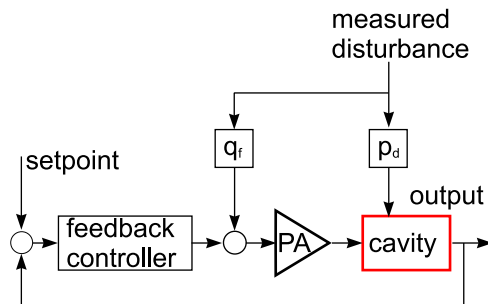


Figure 4.2: Feedback and feed-forward control of the accelerating voltage of a cavity fed by a power amplifier (PA).

5 Optimum External Quality Factor

In accelerators the cavity coupler supplies high RF power from an RF source to a cavity, which transfers this power to the beam via the cavity longitudinal electric field. As we mentioned in the previous section the reflected power completely disappears if the cavity is pre-detuned and the external quality factor is equal to the optimal value (4.8). However, having adjustable couplers in order to minimize the reflected power from each cavity is expensive because of complicated technology. In addition, the adjustable couplers are less reliable so that the couplers with a fixed quality factor will be used in the ESS spoke LINAC. Therefore, we have to choose external Q -factor in such a way that the power reflected by the whole spoke LINAC will be minimal. At the same time, we should keep in mind that the ESS LINAC will be upgraded to accelerate a 75 mA beam and we have to try also to minimize the reflected power for the upgraded case as well. Using the voltage distribution along the spoke LINAC shown in Fig. 3.3 and Eqs. (4.3), (4.4) we have calculated the total reflected power within the steady-state approximation $A(t) = V_c$. The cavity parameters are given in the Table I:

Table I. Beam and spoke cavity parameters.

Parameter	Symbol	Value
DC beam current	I_b^{DC}	50 mA
Accelerating gradient	E_{acc}	8.5 MV
Accelerating length	L_{acc}	0.639 m
Cavity voltage	V_c	5.1 MV
Beam form-factor	F_b	1
Bare cavity Q -factor	Q_0	$1.2 \cdot 10^{10}$
Geometric shunt impedance	R/Q	213 Ω
Frequency	f	352.21 MHz

The Lorentz force detuning is ignored in these simulations. Note that if the beam velocity β is different from the phase velocity of the spoke cavity $\beta_0 = 1/2$, then the geometric shunt impedance (R/Q) in Eqs. (4.3), (4.4) have to be replaced by $(R/Q)T(\beta)$.

From Fig. 5.1 one can see that the power reflected by the spoke LINAC with a 50 mA beam is minimal at $Q_{ext} \approx 2.8 \times 10^5$ whereas the power reflected in the case of a 75 mA beam is minimal at $Q_{ext} \approx 1.9 \times 10^5$. The same absolute level of reflected power is achieved in both cases at

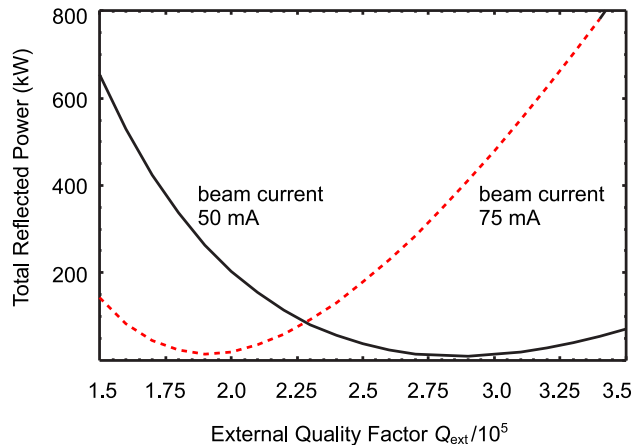


Figure 5.1: The total power reflected by the spoke LINAC vs. the external quality factor. The main and upgraded LINAC configurations with 50 and 75 mA beams are considered

$Q_{ext} \approx 2.3 \times 10^5$ and the minimum ratio of the reflected power to incident one equaling 1.18% is realised at $Q_{ext} \approx 2.34 \times 10^5$. In what follows, the latter value of the external quality factor is used in our simulations of the RF power consumptions in the ESS spoke LINAC. Thus,

$$Q_{ext} = 2.34 \times 10^5. \quad (5.1)$$

6 Simulation of a Single Cavity

In this section we present in detail the simulation results of the dynamics of the first spoke cavity in order to demonstrate the physics of the beam loading, Lorentz force detuning and the cavity voltage and phase stabilization. The analysis of the cavity voltage evolution in the presence of the beam loading and Lorentz detuning governed by Eqs. (4.2)-(4.9) with applied feed-forward and feedback controls is performed with a model developed in the Simulink MatLab in a way similar to that realized in [3]. The RF source is modelled as a current source that emits an incident wave fed to the cavity coupler. The frequency response of the RF source is modelled as a low pass filter with 1 MHz bandwidth. The negative feedback is based on a PID controller that controls a system's output by comparing it to a desired setpoint and feeding the error back to the input dynamically. Since a perturbation caused by the Lorentz detuning is repetitive, a feed-forward technique is used to prevent such a perturbation. Combined feedback and feed-forward control can significantly improve performance over simple feedback architectures when there is a major disturbance to the system that can be measured beforehand [3]. The diagram of a control system is shown in Fig. 4.2. The parameters used for simulations are given in the Table II:

Table II. The parameters of the first spoke cavity and the beam.

Parameter	Symbol	Value
Beam velocity	β	0.386
Cavity voltage	V_c	5.1 MV
Maximum voltage seen by beam	V_b	3.72 MV
Accelerating phase (LINAC convention)	ϕ_s	-28.7 deg
Optimal cavity pre-detuning	Δf^{opt}	258 Hz
External Q -factor	Q_{ext}	$2.34 \cdot 10^5$
Transit-time factor time	T	0.73
Lorentz detuning coefficient	K_L	-2.8 Hz/(MV/m) ²

6.1 cavity without control

Let us first consider the cavity without control but with implemented cavity pre-detuning and a stepwise variation of the incident power shown in Fig. 6.1 that allow to mitigate the beam loading effect. The beam during its passage through the cavity induces the voltage that adds to the voltage induced by the incident (from coupler) current so that the magnitude and phase of the total induced voltage change during the interaction of the beam with the cavity, see Figs. 6.2, 6.3 representing the cavity voltage magnitude and phase as a function of time. Filling of the cavity with an electromagnetic field is also accompanied by the Lorentz detuning shown in Fig. 6.4. The power transferred to the beam is presented in Fig. 6.5. Note that the beam is accelerated off-crest so that it cannot absorb the whole RF power fed to the cavity. In order to prevent the cavity against overcharging in terms of voltage, the incident power is quickly reduced at the moment of beam injection to keep the accelerating voltage at the nominal level of 5.1 V. Hence, the incident power distribution has a stepwise shape. Let us stress that one should distinguish between the voltage seen by the beam and the cavity voltage. The latter corresponds to the voltage seen by a particle traveling with the velocity equaling the phase velocity of the accelerating π -mode. The cavity pre-detuning in terms of frequency is typically used to set the cavity phase to zero. In the simulations shown in Figs. 6.2, 6.3 despite the frequency pre-detuning the cavity phase strongly deviates from zero because the Lorentz force effect is essential.

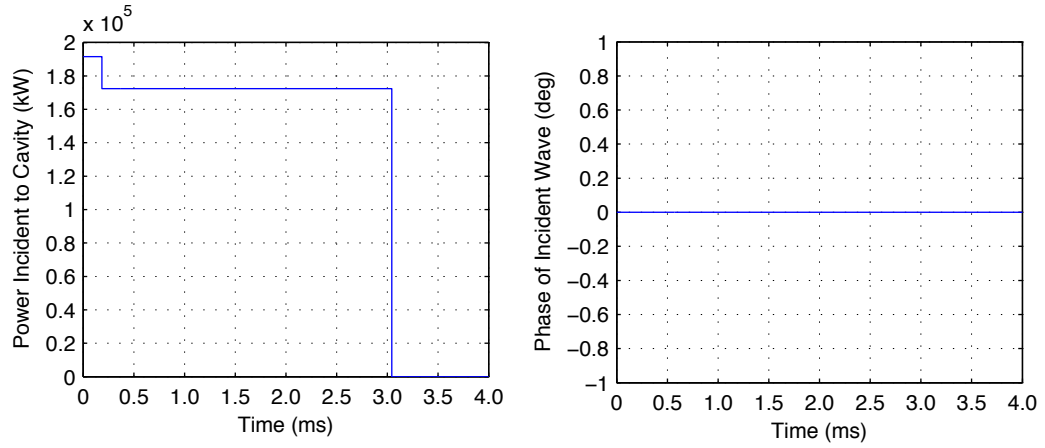


Figure 6.1: The power feed to the cavity (on the left) and the phase of the incident wave (on the right) vs. time. There is no control but the cavity pre-detuning and stepwise variation of the incident power are used.

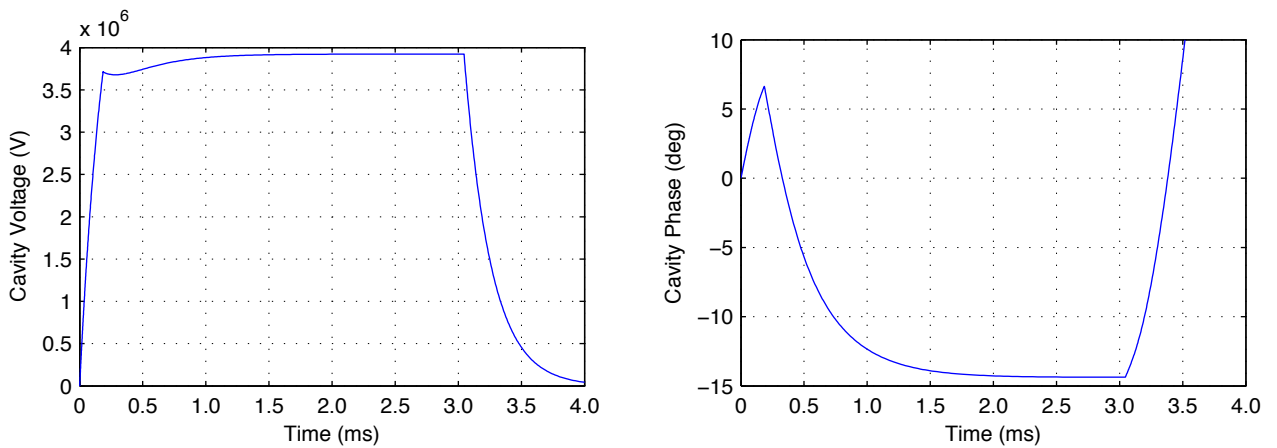


Figure 6.2: The cavity voltage magnitude and phase vs. time.

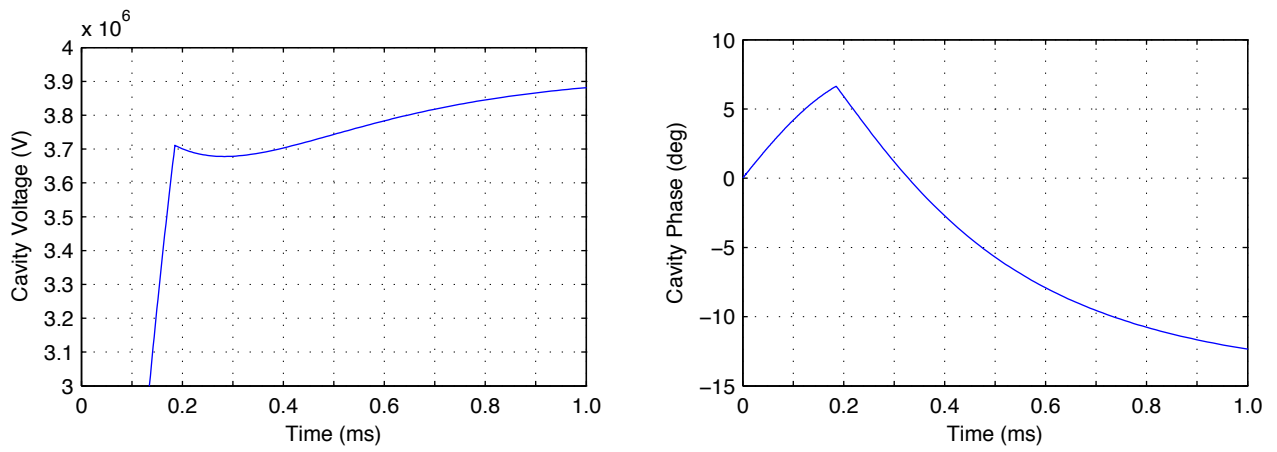


Figure 6.3: Detailed view of the cavity voltage magnitude and phase dynamics around the moment of the beam injection.

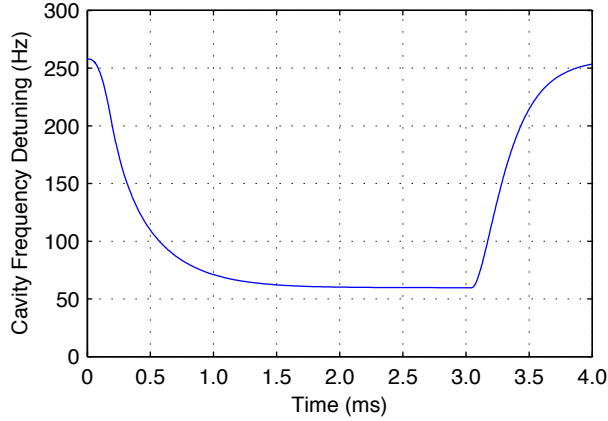


Figure 6.4: Dynamic detuning of the frequency caused by the electromagnetic pressure vs. time.

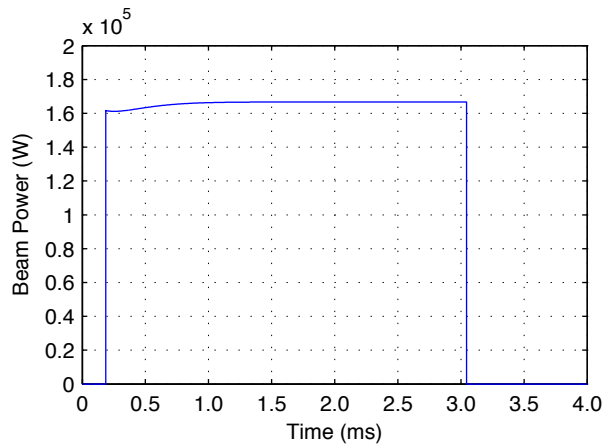


Figure 6.5: The power transferred to the beam vs. time.

6.2 cavity with control but without pre-detuning

We saw that the cavity voltage and phase deviate substantially from the required nominal values. As we mentioned the cavity voltage can be controlled by means of a fast feedback to mitigate the beam loading and by a slow feed-forward to cure the Lorentz detuning. In this subsection we present the simulation results of the cavity dynamics in the presence of control. Note that the feedback and the cavity pre-detuning produce opposite actions. Specifically, the feedback tends to keep the cavity voltage at zero level whereas the pre-detuning creates a phase phase shift that cancels the phase shift caused by the beam loading. So, without beam the feedback effect tries to compensate the pre-detuning effect so that we will first consider the cavity behaviour without applying the pre-detuning. The simulation results for the power required to be fed to the cavity as well as the phase of the incident wave are presented in Fig. 6.6, 6.7. The results for the controlled

cavity voltage and phase are shown in Figs. 6.8 and 6.9. Applying the feed-forward control by means of fast piezo-tuners one can also stabilize the cavity frequency as it is shown 6.10. The feedback regulation response is limited by a delay of a few microseconds such that the cavity phase deviates by around two degrees from the nominal value during the beam injection. As a result, the power transferred to the beam is not well stabilized as one can see in Fig. 6.11. This phase error rising in each cavity is systematic and its cumulative effect strongly degrades the beam quality. In the next subsection we analyse how to reduce this systematic error in phase.

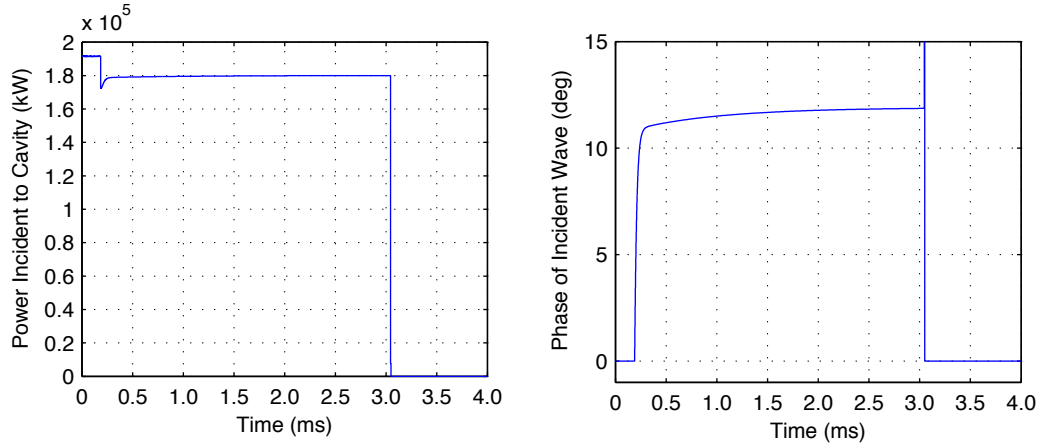


Figure 6.6: The power feed to the cavity (on the left) and the phase of the incident wave (on the right) vs. time. The stepwise variation of the incident power and stabilization control are applied but there is not cavity pre-detuning.

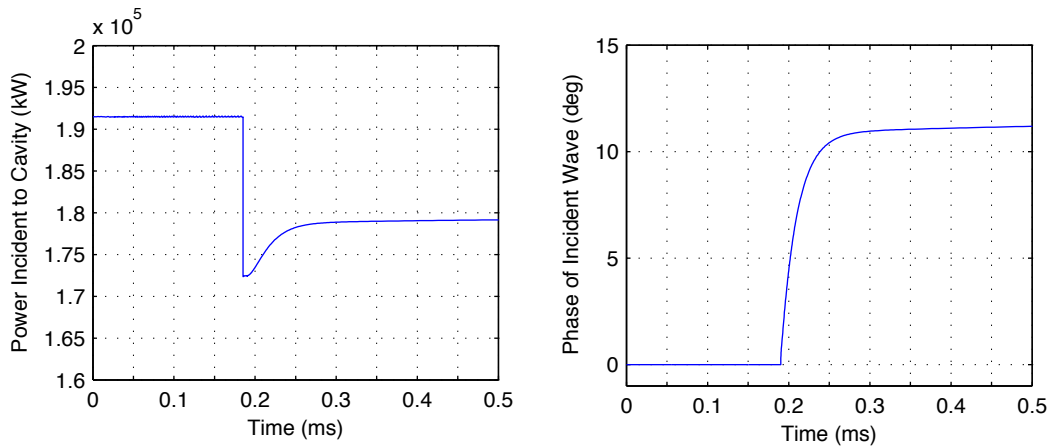


Figure 6.7: Detailed view of the incident power and associated with it phase around the moment of the beam injection. vs. time.

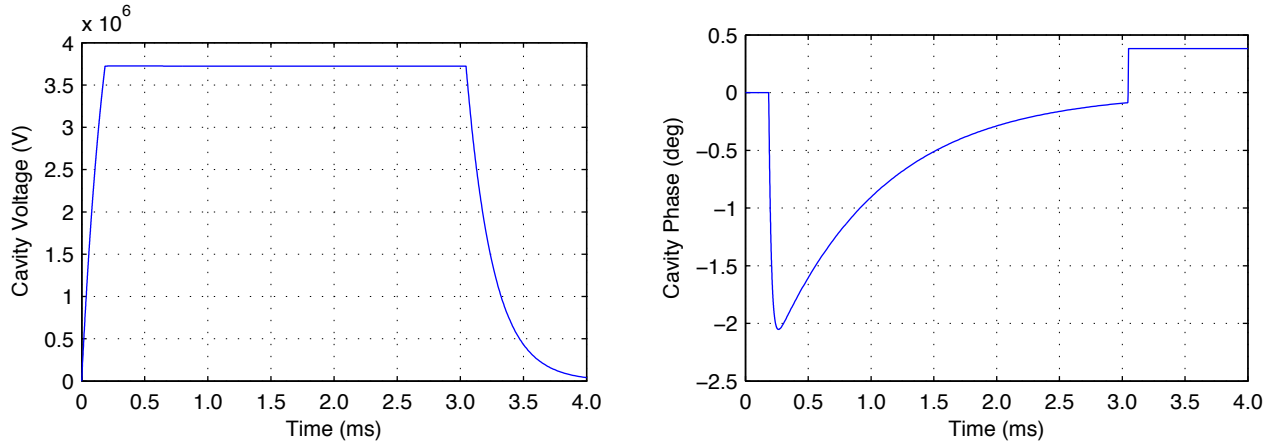


Figure 6.8: The cavity voltage magnitude and phase vs. time.

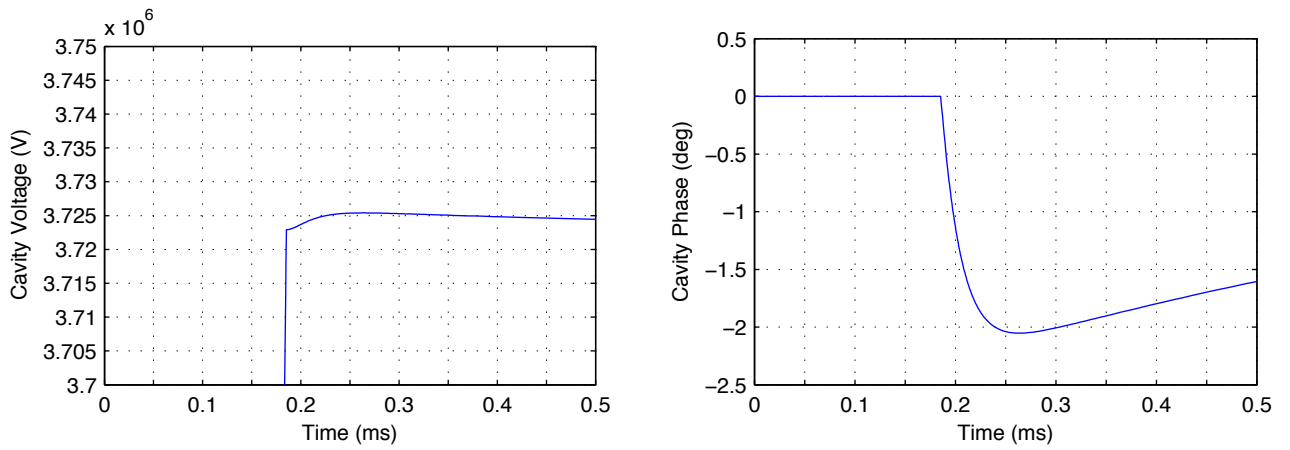


Figure 6.9: Detailed view of the cavity voltage magnitude and phase dynamics around the moment of the beam injection.

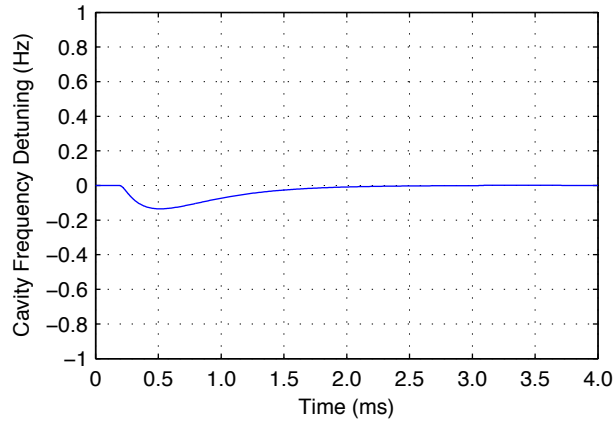


Figure 6.10: Dynamic detuning of the frequency caused by the electromagnetic pressure vs. time.

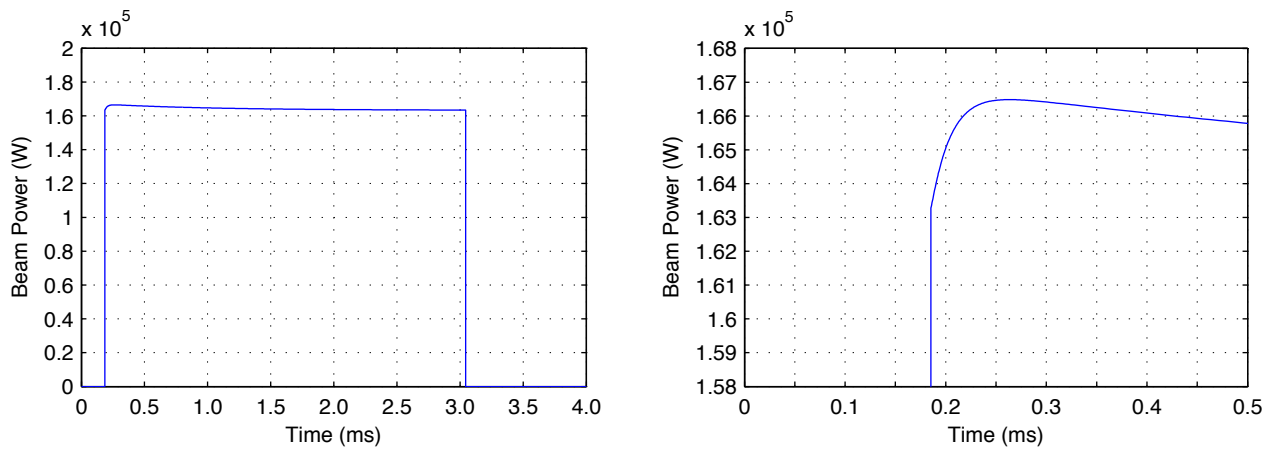


Figure 6.11: The power transferred to the beam vs. time (on the left) and detailed view around the moment of the beam injection (on the right).

6.3 cavity with control and pre-detuning

To mitigate the delay effect and associated with it the phase jump when the beam enters the cavity, we propose to use the cavity pre-detuning technique and turn on the feedback at the generator start-up. Then, without beam the phase shift caused by the pre-detuning is undercompensated by feedback because of delay and this undercompensated phase shift cancels the phase jumps when the beam enters the cavity. As a result, the cavity voltage and phase deviations are stabilized within 20 microseconds with an accuracy of 0.1% and 0.5° , respectively. The incident power, cavity voltage magnitude and phase, the frequency detuning and the beam power as functions of time are shown in Fig. 6.12, 6.13, 6.14, 6.15, 6.16 and 6.17, respectively.

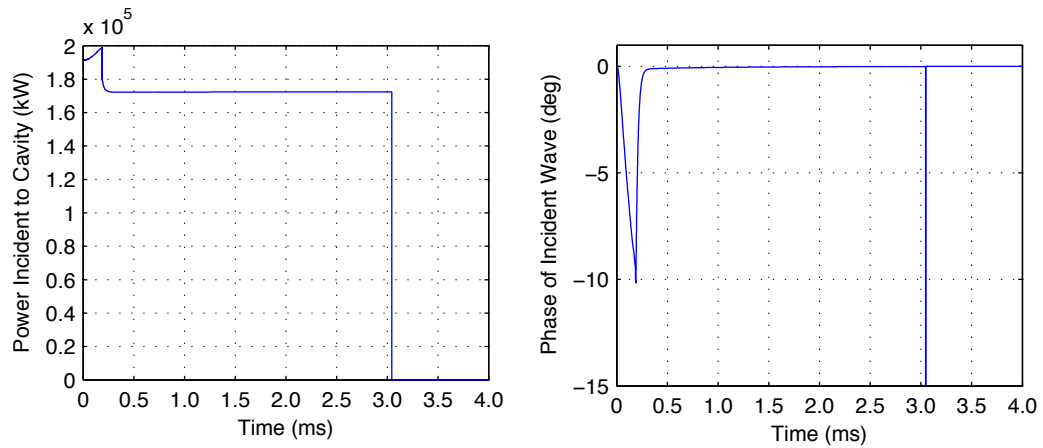


Figure 6.12: The power feed to the cavity (on the left) and the phase of the incident wave (on the right) vs. time. The cavity pre-detuning, stepwise variation of the incident power and stabilization control are applied.

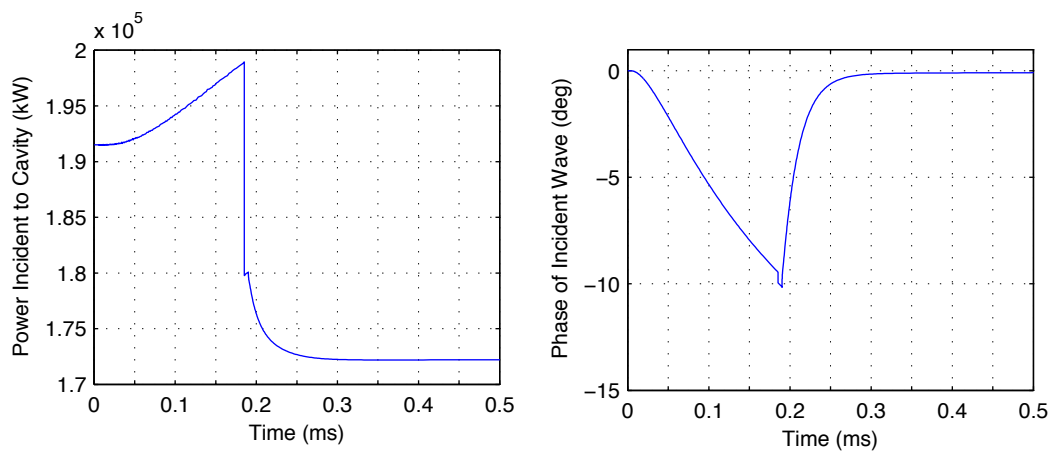


Figure 6.13: Detailed view of the incident power and associated with it phase around the moment of the beam injection. vs. time.

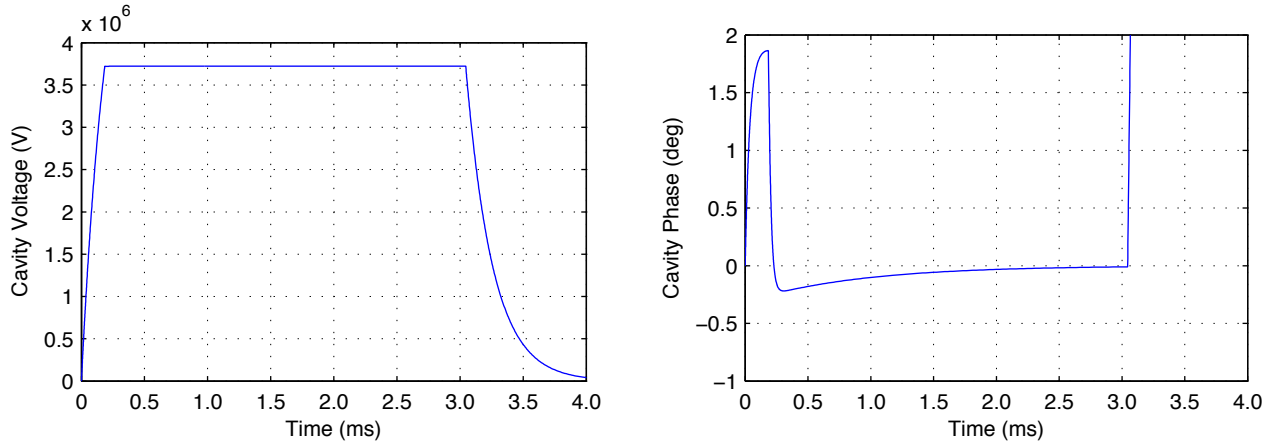


Figure 6.14: The cavity voltage magnitude and phase vs. time.

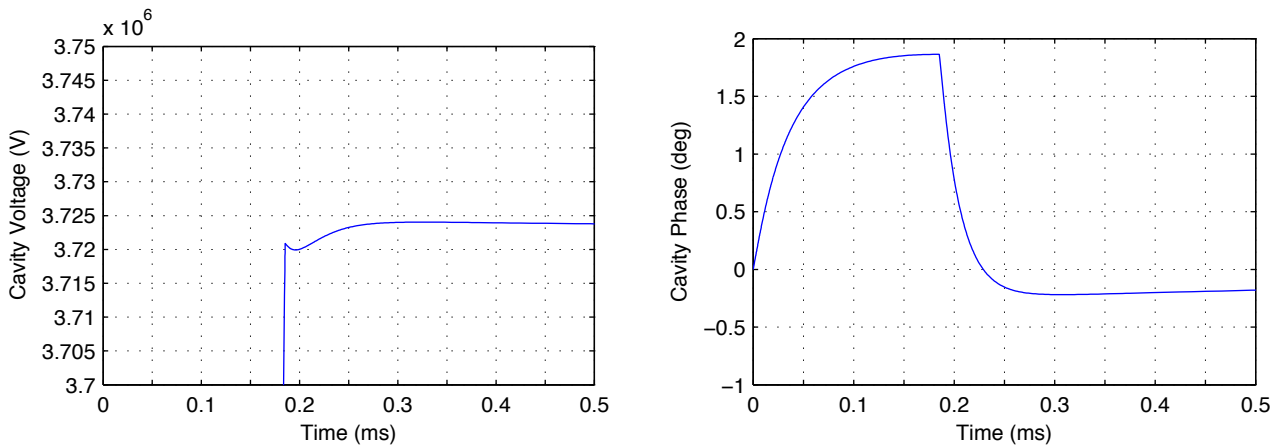


Figure 6.15: Detailed view of the cavity voltage magnitude and phase dynamics around the moment of the beam injection.

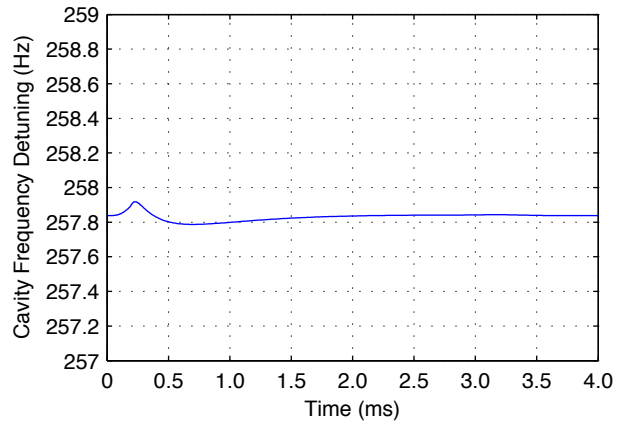


Figure 6.16: Dynamic detuning of the frequency caused by the electromagnetic pressure vs. time.

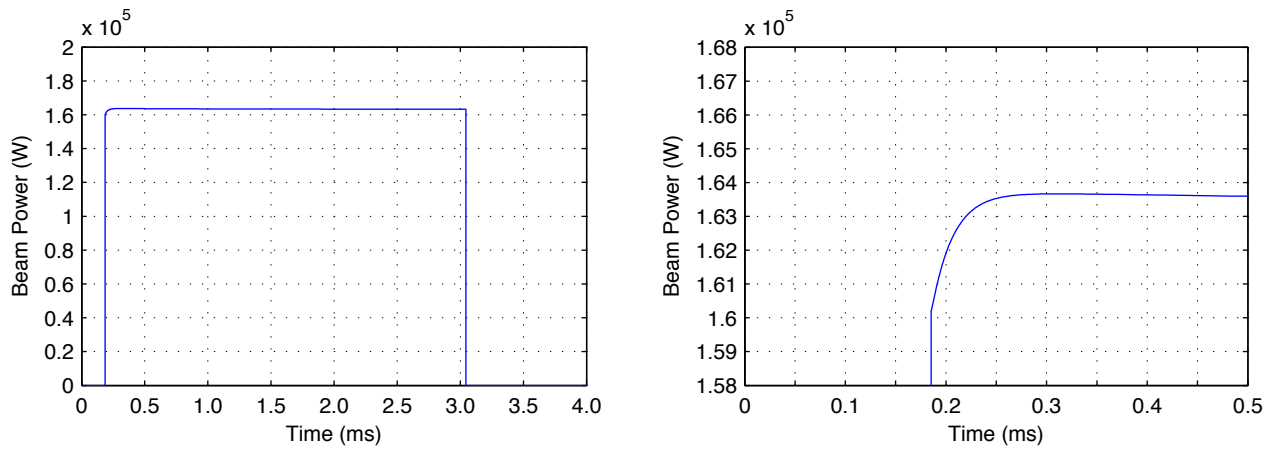


Figure 6.17: The power transferred to the beam vs. time (on the left) and detailed view around the moment of the beam injection (on the right).

7 RF Power Consumption along the Spoke LINAC

Using the Simulink model with implemented feedback and feed-forward one can calculate the voltage and phase dynamics in each cavity of the ESS spoke LINAC in the presence of the beam loading and Lorentz detuning. The peak and averaged (over the pulse) RF power required to be fed from the coupler to the cavity are presented in Fig. 7.1. The power transferred to the beam in each cavity is also presented. In our calculations we considered the worst case when the Lorentz force detuning is not compensated by feed-forward. At the same time, the spoke cavity is stiff and the Lorentz detuning is weak. One can see that in the current design of the ESS spoke LINAC almost all RF power is on average transferred to the beam. But the peak RF power required to compensate the beam loading can exceed the average power by 20% at the beginning of the spoke LINAC because the beam is accelerated substantially off-crest. The simulation results for the upgraded ESS LINAC with a current of 75 mA are shown in Fig. 7.2. Recall that the pulse of incident RF power has a stepwise shape with a peak of a duration around $200 \mu\text{s}$ at the beginning. This peak is followed by the main part of an RF pulse of around 2.86 ms. This main part is substantially smaller in terms of power and only a few per cents higher than the power transferred to the beam. Thus, with the present ESS LINAC design the RF overhead on average is quite low. The maximal power required to the coupler is 260 kW for a 50 mA beam and 410 kW for a 75 mA beam.

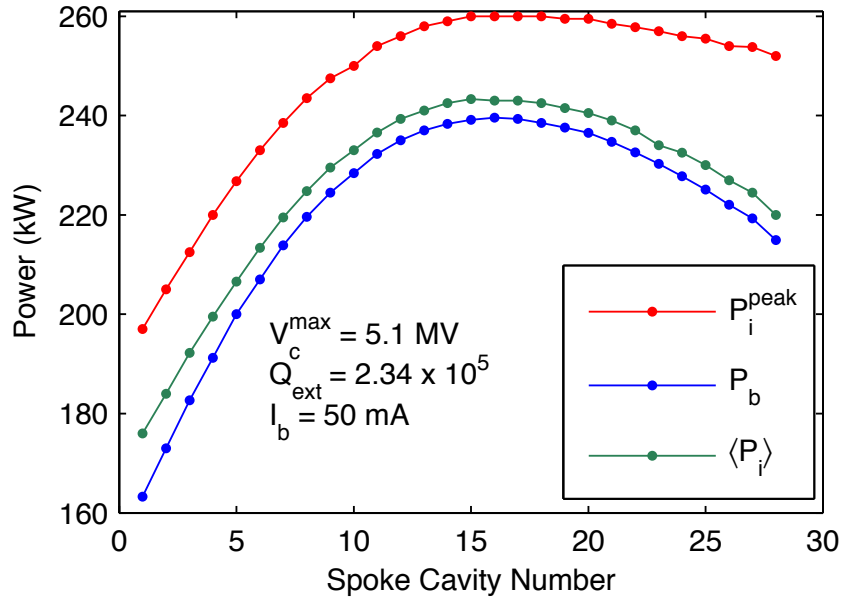


Figure 7.1: The incident peak (red curve) and average (green curve) power to be fed to each spoke cavity coupler for 50 mA beam current are shown. The power transferred to the beam in each cavity is represented by the blue curve.

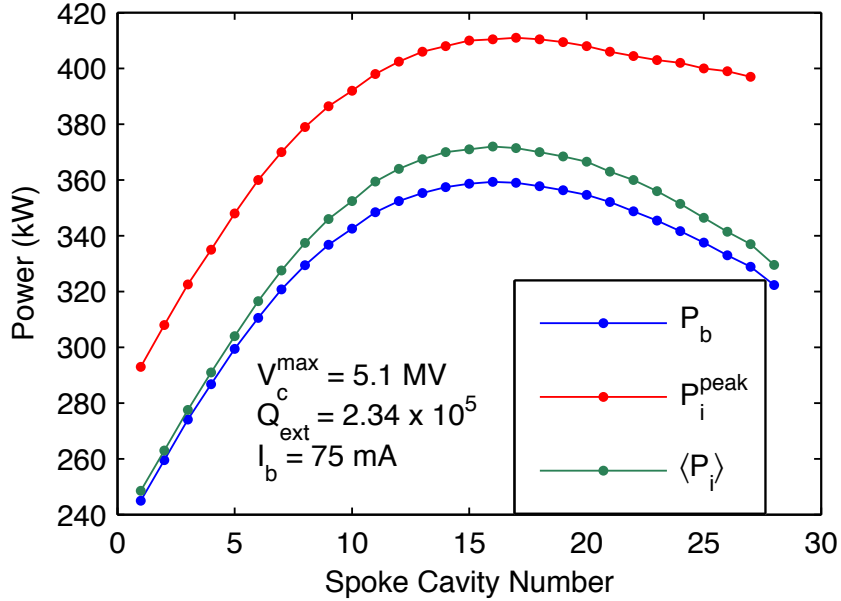


Figure 7.2: The incident peak (red curve) and average (green curve) power to be fed to each spoke cavity coupler for 75 mA beam current are shown. The power transferred to the beam in each cavity is represented by the blue curve.

8 Conclusion

It turns out that using the cavity pre-detuning, stepwise variation of the incident power and feedback as well as feed-forward control one can stabilize the voltage magnitude and phase on the nominal level within 20 μs whereas without the cavity pre-detuning the phase stabilization can not be achieved because of feedback loop delay.

The power overhead is mainly dictated by the beam loading because of high beam current. Therefore, the substantial power overhead lasts only around 200 microseconds but the ratio of the peak power to the average power is significant and reaches 20% at the beginning of the spoke LINAC. This significant overhead at the beginning is the result of mismatch between the beam velocity and cavity phase velocity so that the transmission line is also mismatched to the cavity. In addition, at the beginning of the spoke LINAC the beam loading is also stronger because of higher value of the synchronous phase (i.e. deviation from the on-crest acceleration is stronger). In the present ESS LINAC design the RF overhead on average is quite low. The maximum power required to the coupler is 260 kW for a 50 mA beam and 410 kW for a 75 mA beam. Taking into account an additional safety margin of 15% to compensate for RF losses in a distribution line and RF source regulation ², we expect that the RF source proving up to 300 kW for a 50 mA beam case and 450 kW for a 75 mA beam is suitable to drive the spoke cavities.

The authors would like to acknowledge S. Bousson who provided the electric field distribution of the double spoke cavity.

²typically the klystron requires around 20% of the RF power overhead but by applying the linearization technique this overhead can be reduced

References

- [1] S. Peggs, ‘Conceptual Design Report,’ ESS-2012-001, 2012.
- [2] S. Molloy ‘Linac power optimisation including beam-velocity effects,’ ESS report: January 25, 2012.
- [3] M. Hernandez, W. Höfle, sLHC Project Report 0054, CERN, April 2001.
- [4] H. Padamsee ‘RF superconductivity,’ WILEY VCH, 2009, 448 p.
- [5] K.W. Shepard, P.N. Ostroumov, J.R. Delayen, ‘High-energy ion linacs based on superconducting spoke cavities,’ Phys. Rev. ST Accel. Beams 6, 080101 (2003).
- [6] M. Eshraqi et al. ‘Design and beam dynamics study of hybrid ESS LINAC,’ IPAC11, WEPS062, 2011.
- [7] S. Peggs, R. Kreier, ‘ESS Technical Design Report,’ release 1.0, Nov. 27, 2012.
- [8] J. Tückmantel, ‘Cavity-Beam-Transmitter Interaction Formula Collection with Derivation.’ Internal Note, CERN-ATS-NOTE-2011-002 TECH.
- [9] M. Doleans, ‘Studies in reduced-beta elliptical superconducting cavities,’ PhD, 2003.